

A Recursive Network with Dynamic Attention for Monaural Speech Enhancement

Andong Li^{1,3}, Chengshi Zheng^{1,3}, Cunhang Fan^{2,3}, Renhua Peng^{1,3}, Xiaodong Li^{1,3}

¹ Key Laboratory of Noise and Vibration Research, Institute of Acoustics, Chinese Academy of Sciences, Beijing, China

² NLPR, Institute of Automation, Chinese Academy of Sciences, Beijing, China

³ University of Chinese Academy of Sciences, Beijing, China

{liandong, cszheng, pengrenhua, lxd}@mail.ioa.ac.cn, cunhang.fan@nlpr.ia.ac.cn

Abstract

A person tends to generate dynamic attention towards speech under complicated environments. Based on this phenomenon, we propose a framework combining dynamic attention and recursive learning together for monaural speech enhancement. Apart from a major noise reduction network, we design a separated sub-network, which adaptively generates the attention distribution to control the information flow throughout the major network. To effectively decrease the number of trainable parameters, recursive learning is introduced, which means that the network is reused for multiple stages, where the intermediate output in each stage is correlated with a memory mechanism. As a result, a more flexible and better estimation can be obtained. We conduct experiments on TIMIT corpus. Experimental results show that the proposed architecture obtains consistently better performance than recent state-of-the-art models in terms of both PESQ and STOI scores. The code is provided at <https://github.com/Andong-Li-speech/DARC�>.

Index Terms: monaural speech enhancement, recursive learning, attention U-Net, dynamic attention

1. Introduction

In real environments, clean speech is often contaminated by background interference, which may significantly reduce the performance of automatic speech recognition [1], speaker verification [2] and hearing aids [3]. Monaural speech enhancement aims to extract the target speech from the mixture when only one-microphone is available [4]. In recent years, deep neural networks (DNNs) have shown their promising performance on monaural speech enhancement even in highly non-stationary noise environments owing to their superior capability in modeling the complex nonlinearity [5]. Typical DNN-based methods can be categorized into two classes according to estimation targets, where one is masking-based [6] and the other is spectral mapping-based [7].

Previous DNNs usually adopted fully-connected (FC) layers for noise reduction [6, 7]. To tackle the speaker generalization problem, Chen *et al.* proposed to utilize stacked long short-term memory (SLSTM) [8], which significantly outperformed DNNs. Recently, various convolutional neural networks (CNNs) with complex topology were proposed [9, 10, 11, 12] and achieved consistently better performance than SLSTM and meanwhile, dramatically decreased the number of trainable parameters. More recently, Tan *et al.* combined convolutional auto-encoder (CAE) [13] and LSTM together and proposed convolutional recurrent neural network (CRN) [14], where CAE helped to learn temporal-frequency (T-F) patterns and LSTM effectively captured dynamic sequence correlations.

Despite a variety of models with complex topologies have been proposed recently [10, 11, 12, 14], which have achieved state-of-the-art performance, they still have limitations and are attributed as two-fold. For one thing, the number of the parameters is often partly limited to meet the low-latency requirement, which heavily restricts the depth of the network. For another, the increase of depth is more likely to cause a gradient vanishing problem. Recently, progressive learning is proposed [15, 16], which decomposes the mapping process into multiple stages. The results show that it dramatically decreases the number of trainable parameters and effectively maintains the performance [16]. Based on the conception, recursive learning [17] is proposed by reusing the network for multiple stages, where the output in each stage is linked by a memory mechanism. It further alleviates the parameter burden and deepens the network without introducing extra parameters.

Human tends to generate adaptive attention with dynamic neuron circuits to percept complicated environments [18]. For example, when a person hears an utterance from the real environments, the more noise components are dominant, the more neuron attentions are needed to figure out the meaning and vice versa. This phenomenon reveals the dynamic mechanism of auditory perception system. Motivated by the physiological phenomenon, we propose a novel network combining dynamic attention and recursive learning together. Different from the previous networks [10, 11, 12, 14] that a single complex network is designed for the task, the framework encompasses a major network and an auxiliary sub-network in parallel, where the one is noise reduction module (NRM) and the other is attention generator module (AGM). The workflow of the framework is as follows: At each intermediate stage, both the noisy feature and the estimation from the last stage are combined into the current input. AGM is adopted to generate the attention set, which is subsequently applied to NRM through the pointwise convolution and sigmoid function. In this way, AGM actually serves as a type of perception module to flexibly adjust the weight distribution of NRM, leading to better performance for noise suppression. To our best knowledge, it is the first time for a dynamic attention mechanism to be proposed for speech enhancement.

The remainder of the paper is structured as follows. Section 2 formulates the problem. The architecture of the network is illustrated in Section 3. Section 4 is the dataset and experimental settings. Section 5 presents the results and analysis. Section 6 draws some conclusions.

2. Problem formulation and notation

In the time domain, a noisy signal can be modeled as $x(n) = s(n) + d(n)$, where n is the discrete time index. With short-time Fourier transform (STFT), it can be further rewritten as:

$$X_{k,l} = S_{k,l} + D_{k,l}, \quad (1)$$

where $X_{k,l}$, $S_{k,l}$, and $D_{k,l}$ respectively refer to the noisy, clean, and noise components at the frequency bin index k and the time frame index l . In this study, the network is deployed to estimate the magnitude of spectrum (MS), which is then incorporated with noisy phase to recover the estimated spectrum. Inverse short-time Fourier transform (iSTFT) is used to reconstruct the waveform in the time domain.

For simplicity of notation, we define the principal notations used in this paper. $|\mathbf{X}| \in \mathbb{R}^{T \times F}$, $|\mathbf{S}| \in \mathbb{R}^{T \times F}$, $|\tilde{\mathbf{S}}^l| \in \mathbb{R}^{T \times F}$, and $|\hat{\mathbf{S}}^l| \in \mathbb{R}^{T \times F}$ denote the magnitude of noisy spectrum, the magnitude of clean spectrum, the estimated magnitude of spectrum in l th stage, and the final estimated magnitude of spectrum, respectively. T and F refer to the timestep and feature length. As recursive learning is used, superscript l denotes the stage index, and the number of stages is notated as Q .

3. Architecture illustration

3.1. Stage recurrent neural network

SRNN is first proposed in [17], which is the core component in recursive learning. It is capable of aggregating the information across different stages with a memory mechanism, which is comprised of two parts, namely two-dimensional convolutional (2-D Conv) block and convolutional-RNN (Conv-RNN) block. The first part tries to project the input features into a latent representation, followed by Conv-RNN to update the state in the current stage. Assuming the output of 2-D Conv and Conv-RNN at stage l are respectively notated as $\hat{\mathbf{h}}^l$ and \mathbf{h}^l , the inference of SRNN is formulated as:

$$\hat{\mathbf{h}}^l = f_{conv}(|\mathbf{X}|, |\tilde{\mathbf{S}}^{l-1}|), \quad (2)$$

$$\mathbf{h}^l = f_{conv.rnn}(\hat{\mathbf{h}}^l, \mathbf{h}^{l-1}), \quad (3)$$

where f_{conv} and $f_{conv.rnn}$ refer to the functions of 2-D Conv and Conv-RNN, respectively. \mathbf{h}^{l-1} is the state of the last stage. In this study, ConvGRU [19] is adopted as the unit in Conv-RNN, whose calculation process gives as follows:

$$\mathbf{z}^l = \sigma(\mathbf{W}_z^l \otimes \hat{\mathbf{h}}^l + \mathbf{U}_z^l \otimes \mathbf{h}^{l-1}), \quad (4)$$

$$\mathbf{r}^l = \sigma(\mathbf{W}_r^l \otimes \hat{\mathbf{h}}^l + \mathbf{U}_r^l \otimes \mathbf{h}^{l-1}), \quad (5)$$

$$\mathbf{n}^l = \tanh(\mathbf{W}_n^l \otimes \hat{\mathbf{h}}^l + \mathbf{U}_n^l \otimes (\mathbf{r}^l \odot \mathbf{h}^{l-1})), \quad (6)$$

$$\mathbf{h}^l = (\mathbf{1} - \mathbf{z}^l) \odot \hat{\mathbf{h}}^l + \mathbf{z}^l \odot \mathbf{n}^l, \quad (7)$$

where \mathbf{W} and \mathbf{U} represent the weight matrices of the cell. $\sigma(\cdot)$ and $\tanh(\cdot)$, respectively, denote the sigmoid and the tanh activation functions. \otimes represents the convolutional operator and \odot is the element-wise multiplication. Note that biases are ignored for notation convenience.

3.2. Attention gate

AU-Net is first proposed in [20] to improve the accuracy in the segmentation-related tasks, where attention gates (AGs) are inserted between the convolutional encoder and the decoder. Compared with a standard U-Net, AU-Net has the capability of

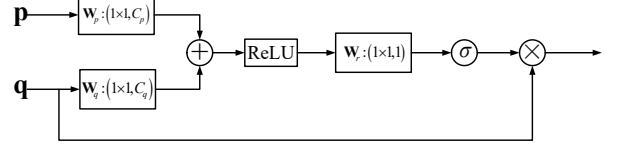


Figure 1: The structure of attention gate adopted in NRM. \mathbf{p} and \mathbf{q} refer to the feature of a decoding layer and its corresponding feature in an encoding layer, respectively. \mathbf{W}_p , \mathbf{W}_q and \mathbf{W}_r are 2-D convolutional layers, whose kernel size are 1×1 . C_p and C_q refer to the channel numbers of \mathbf{p} and \mathbf{q} . Batch normalization is used after each convolutional operation.

automatically suppressing the irrelevant regions and emphasizing the important features. As the spectrum includes abundant frequency components, where formants are often dominant in the low-frequency regions and the regions of the high-frequency have a sparse distribution, it is necessary to discriminate different spectral regions with different weights. The schematic of the AG adopted in this paper is shown in Fig. 1. Assuming the inputs of the unit are \mathbf{p} and \mathbf{q} , where \mathbf{p} and \mathbf{q} refer to the feature of a decoding layer and its corresponding feature in an encoding layer, respectively. the output can be calculated as:

$$\mathbf{y} = \mathbf{q} \odot \sigma(\mathbf{W}_r \otimes \text{ReLU}(\mathbf{W}_p \otimes \mathbf{p} + \mathbf{W}_q \otimes \mathbf{q})), \quad (8)$$

where \mathbf{W}_p , \mathbf{W}_q and \mathbf{W}_r are the convolution kernels. Note that the unit consists of two branches, where the one merges the information of both inputs and generates the attention coefficients through a sigmoid function and the other copy the information of \mathbf{q} and multiply the coefficients. After the output of AG is obtained, it is concatenated with the feature from the corresponding decoding layer along the channel dimension as the input of the next decoding layer.

3.3. Proposed architecture

The overview of the proposed architecture is depicted in Fig. 2-(a). It encompasses two modules, namely AGM and NRM, and the two modules are designed to interleave execution during the whole process. The architecture is operated with a recursive procedure, i.e., the whole forward stream can be unfolded into multiple stages. In each stage, the original noisy spectrum and the estimation from the last stage are concatenated, serving as the network input. It is sent to AGM to generate the current attention set, representing the attention distribution at the current stage. It is subsequently applied to NRM to control the information flow throughout the network. NRM also receives the input to estimate the MS. As a consequence, the output of AGM dynamically depends on how well MS is estimated in the last stage, i.e., AGM is capable of re-weighting the attention distribution according to the previous feedback from the noise reduction system.

Assuming the mapping functions of AGM and NRM are denoted as G_A and G_R , respectively. The calculation procedure of the proposed architecture works as follows:

$$\mathbf{a}^l = G_A(|\mathbf{X}|, |\tilde{\mathbf{S}}^{l-1}|; \theta_A), \quad (9)$$

$$|\tilde{\mathbf{S}}^l| = G_R(|\mathbf{X}|, |\tilde{\mathbf{S}}^{l-1}|, \mathbf{a}^l; \theta_R), \quad (10)$$

where \mathbf{a} is the generated attention set. θ_A and θ_R represent the network parameters for AGM and NRM.

In this study, we use a typical U-Net [21] topology for AGM, which consists of the convolutional encoder and the decoder. The encoder consists of five successive 2-D convolutional layers, each of which is followed by batch normalization (BN) [22] and exponential linear unit (ELU) [23]. The number

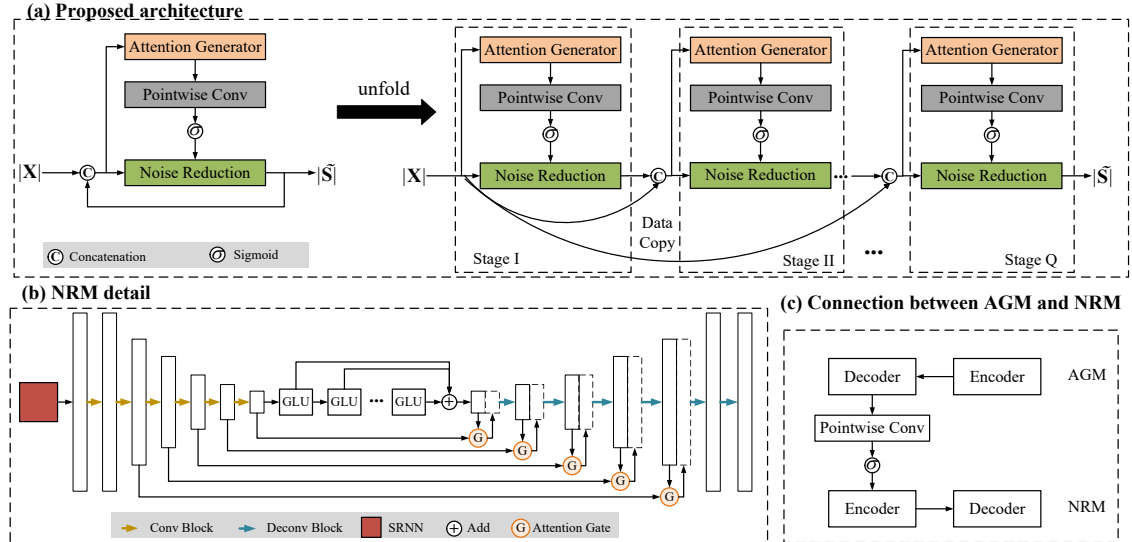


Figure 2: The schematic of proposed architecture. (a) Proposed architecture and its unfolding structure. The architecture encompasses two parts in parallel, namely AGM and NRM. (b) The detailed structure of NRM. (c) The connection between AGM and NRM.

of channels through the encoder is (16, 32, 32, 64, 64). The decoder is the mirror representation of the encoder except all the convolutions are replaced by deconvolutions [24] to effectively enlarge the mapping size. Similarly, the number of channels through the decoder is (64, 64, 32, 32, 16). The kernel size, stride for both encoder and decoder are (2, 5) and (1, 2), respectively. Skip connections are introduced to compensate for information loss during the encoding process.

The detail of NRM is shown in Fig. 2-(b). It includes three parts, namely SRNN, AU-Net and a series of GLUs [10]. Given the input of the network, whose size is $T \times F \times 2$. 161 is the feature length, and 2 is the number of the input channel. The output size after SRNN and consecutive six convolutional blocks are $T \times 4 \times 64$. It is subsequently reshaped into $T \times 256$. six concatenated GLUs proposed by [10] are set to explore the contextual correlations efficiently. The output of GLUs is reshaped back to $T \times 4 \times 64$, which is subsequently sent to the decoder to expand the feature size and estimate the MS. The number of channels for the encoder and decoder in AU-Net are (16, 16, 32, 32, 64, 64) and (64, 32, 32, 16, 16, 1), respectively. The kernel size and stride in NRM are the same as the setup in AGM except for the last layer, which takes the pointwise convolution, followed by Softplus as the nonlinearity [25] to obtain the MS. Note that different from direct skip connections in a standard U-Net, the feature mappings from the encoder are multiplied with the gating coefficients from the AGs before they are concatenated with the decoding features, which help to weigh the feature importance in multiple encoding layers.

The connection between AGM and NRM is shown in Fig. 2-(c), where each of the middle features in the decoder of AGM is multiplied to the corresponding feature in the encoder of NRM through the pointwise convolution and the sigmoid function. Note that the sigmoid function is applied to range the value scale into (0, 1).

3.4. Loss function

As the network is trained for multiple stages, at each of which we obtain an intermediate estimation, the accumulated loss can be defined as $\mathcal{L} = \sum_{l=1}^Q \lambda_l \mathcal{D}^l(\hat{S}^l, S)$, where λ_l is the weighted coefficient for each stage, $\mathcal{D}^l(\cdot)$ is the loss function

for l th stage. We set λ_l as 1 in this study, i.e., the same emphasis is given to each training stage.

4. Experimental setup

4.1. Dataset

The experiments are conducted on TIMIT corpus [26]. 4856, 800 and 100 clean utterances are selected for training, validation and testing, respectively. Training and validation dataset are created under the SNR levels ranging from -5dB to 10dB with the interval 1dB whilst we test the model under the SNR conditions of (-5dB, 0dB, 5dB, 10dB). 130 types of noises used in [17] are for training and validation. Another 5 types of noises from NOISEX92 (babble, f16, factory2, m109 and white) are used to explore the generalization capacity of networks. All the collected noises are first concatenated into a long vector. During each mixed process, a random cutting point is generated, which is subsequently mixed with an utterance under an SNR level. As a result, we create 40,000, 4000, 800 noisy-clean pairs for training, validation and testing, respectively.

4.2. Baselines

In this study, four networks are selected as the baselines, namely SLSTM [8], CRN [14], GRN [10] and DCN [12], all of which have achieved state-of-the-art performance recently. For SLSTM, four LSTM layers with 1024 units are stacked, followed by one FC layer to obtain the MS. The input of SLSTM includes the concatenation of the current frame and the previous ten frames. CRN is a type of real-time architecture combining CNN and LSTM. GRN and DCN are typical fully-convolutional network with gating mechanism.

4.3. Parameter setup

All the utterances are sampled at 16kHz. The 20ms Hamming window is applied, with 10ms overlap in adjacent frames. 320-point STFT is adopted, leading to a 161-D feature vector in each frame. All the models are trained with mean-square error (MSE) criterion, optimized by Adam [27]. The learning rate is initialized at 0.001, we halve the learning rate when consecutive 3 validation loss increment happens and the training is early-stopped when 10 validation loss increment happens. All the models are trained for 50 epochs. The minibatch is set to 4

Table 1: Experimental results under seen noise cases. **BOLD** indicates the best result for each case. The number of stage $Q = 3$ for proposed architecture.

Metric	PESQ					STOI (in %)				
	-5dB	0dB	5dB	10dB	Avg.	-5dB	0dB	5dB	10dB	Avg.
Noisy	1.46	1.76	2.14	2.55	1.98	62.44	71.55	81.81	89.53	76.33
SLSTM	2.35	2.67	2.98	3.21	2.80	80.16	86.64	91.24	94.18	88.06
CRN	2.42	2.74	3.06	3.34	2.89	81.45	88.09	92.60	95.57	89.43
GRN	2.47	2.76	3.04	3.25	2.88	82.94	88.63	92.76	95.43	89.94
DCN	2.41	2.75	3.06	3.31	2.88	80.64	87.40	92.10	95.03	88.79
Proposed ($Q = 3$)	2.60	2.91	3.21	3.46	3.05	83.74	89.07	93.17	95.79	90.44

Table 2: Experimental results under unseen noise cases. **BOLD** indicates the best result for each case. The number of stage $Q = 3$ for proposed architecture.

Metric	PESQ					STOI (in %)				
	-5dB	0dB	5dB	10dB	Avg.	-5dB	0dB	5dB	10dB	Avg.
Noisy	1.47	1.83	2.13	2.51	1.98	60.15	72.51	81.23	89.77	75.92
SLSTM	2.07	2.50	2.82	3.12	2.63	74.23	84.52	89.69	93.51	85.49
CRN	2.20	2.60	2.92	3.21	2.73	77.10	86.19	91.03	94.79	87.28
GRN	2.29	2.63	2.89	3.16	2.74	78.10	86.92	91.28	94.78	87.77
DCN	2.20	2.62	2.94	3.22	2.74	76.05	85.88	90.73	94.48	86.78
Proposed ($Q = 3$)	2.37	2.75	3.06	3.34	2.88	79.16	87.54	91.61	95.02	88.33

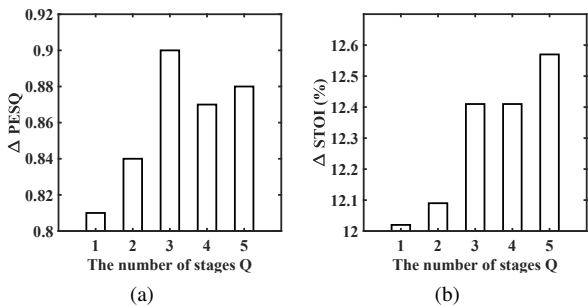


Figure 3: The impact of the number of stages Q . (a) PESQ improvement for different Q . (b) STOI improvement for different Q . All the values are evaluated for unseen noise cases and averaged over different SNRs.

at an utterance level. Within a minibatch, the utterance whose timestep is less than the longest one is padded with zero.

5. Results and analysis

We evaluate the performance of different models with perceptual evaluation speech quality (PESQ) [28] and short-time objective intelligibility (STOI) [29].

5.1. Objective results

Tables 1 and 2 give the results of different models for seen and unseen noise cases, respectively. From the tables, one can observe the following phenomena. Firstly, CRN, GRN, DCN, and proposed model consistently outperform SLSTM in both seen and unseen noise cases. This is because SLSTM solely considers the sequence correlations but neglecting the implicit T-F patterns, which is crucial for spectrum recovery. Moreover, stacked LSTM tends to cause an attenuation effect due to the gradient vanishing problem, which limits the performance. Secondly, compared with the baselines, the proposed architecture obtains notable improvements in both metrics. For example, when going from CRN to the proposed model, PESQ is improved by 0.16 and STOI is improved by 1.01% on average for seen cases. A similar trend is also observed for unseen cases, indicating that the proposed model has a good noise generalization capability. Thirdly, we observe that GRN and DCN achieve close performance. This can be explained as both networks have similar

Table 3: The number of trainable parameters among different models. The unit is million. **BOLD** denotes the lowest trainable parameters.

Model	SLSTM	CRN	GRN	DCN	Proposed
Para. (million)	36.81	17.58	3.13	2.92	1.23

topology, where dilation convolutions combined with the gating mechanism are applied for sequence modeling.

5.2. Impact of stages

We study the impact of the number of stages Q , which is given in Fig. 3. One can get that with the increase of Q , both values of PESQ and STOI are consistently improved when $Q \leq 3$. This indicates that SRNN can effectively refine the performance of the network by a memory mechanism. We also find that when Q increases from 3 to 5, PESQ value slightly degrades whilst STOI is still improved. This is because the distance-based loss like MSE is utilized as the loss function and the optimization process cannot guarantee consistent optimization for both metrics, which is consistent with the previous conclusion in [17].

5.3. Parameter comparison

Table 3 summarizes the number of trainable parameters for different models. One can see that the proposed model dramatically decreases the number of trainable parameters compared with other baselines. This demonstrates the superior parameter efficiency of the proposed architecture.

6. Conclusions

In a complicated scenario, a person usually dynamically adjusts the attention to the change of the environments. Based on the phenomenon, we propose a framework combining dynamic attention and recursive learning. To adaptively control the information flow of the noise reduction network, a separate sub-network is designed to update the attention representation in each stage and is subsequently applied to the major network. As a recursive paradigm is taken for training, the network is reused for multiple stages. As a result, we achieve a refined estimation stage by stage. Experimental results show that compared with previous state-of-the-art models, the proposed model achieves consistently better performance while further decreasing the parameter burden.

7. References

- [1] A. Graves, A.-r. Mohamed, and G. Hinton, "Speech recognition with deep recurrent neural networks," in *2013 IEEE international conference on acoustics, speech and signal processing*. IEEE, 2013, pp. 6645–6649.
- [2] D. A. Reynolds, T. F. Quatieri, and R. B. Dunn, "Speaker verification using adapted gaussian mixture models," *Digital signal processing*, vol. 10, no. 1-3, pp. 19–41, 2000.
- [3] H. Dillon, *Hearing aids*. Hodder Arnold, 2008.
- [4] P. C. Loizou, *Speech enhancement: theory and practice*. CRC press, 2013.
- [5] D. Wang and J. Chen, "Supervised speech separation based on deep learning: An overview," *IEEE/ACM Transactions on Audio, Speech, and Language Processing*, vol. 26, no. 10, pp. 1702–1726, 2018.
- [6] Y. Wang, A. Narayanan, and D. Wang, "On training targets for supervised speech separation," *IEEE/ACM transactions on audio, speech, and language processing*, vol. 22, no. 12, pp. 1849–1858, 2014.
- [7] Y. Xu, J. Du, L.-R. Dai, and C.-H. Lee, "A regression approach to speech enhancement based on deep neural networks," *IEEE/ACM Transactions on Audio, Speech, and Language Processing*, vol. 23, no. 1, pp. 7–19, 2014.
- [8] J. Chen, Y. Wang, S. E. Yoho, D. Wang, and E. W. Healy, "Large-scale training to increase speech intelligibility for hearing-impaired listeners in novel noises," *The Journal of the Acoustical Society of America*, vol. 139, no. 5, pp. 2604–2612, 2016.
- [9] S.-W. Fu, T.-Y. Hu, Y. Tsao, and X. Lu, "Complex spectrogram enhancement by convolutional neural network with multi-metrics learning," in *2017 IEEE 27th International Workshop on Machine Learning for Signal Processing (MLSP)*. IEEE, 2017, pp. 1–6.
- [10] K. Tan, J. Chen, and D. Wang, "Gated residual networks with dilated convolutions for monaural speech enhancement," *IEEE/ACM transactions on audio, speech, and language processing*, vol. 27, no. 1, pp. 189–198, 2018.
- [11] A. Pandey and D. Wang, "TCNN: Temporal convolutional neural network for real-time speech enhancement in the time domain," in *ICASSP 2019-2019 IEEE International Conference on Acoustics, Speech and Signal Processing (ICASSP)*. IEEE, 2019, pp. 6875–6879.
- [12] S. Pirhossainloo and J. S. Brumberg, "Monaural speech enhancement with dilated convolutions," *Proc. Interspeech 2019*, pp. 3143–3147, 2019.
- [13] V. Badrinarayanan, A. Handa, and R. Cipolla, "Segnet: A deep convolutional encoder-decoder architecture for robust semantic pixel-wise labelling," *arXiv preprint arXiv:1505.07293*, 2015.
- [14] K. Tan and D. Wang, "A convolutional recurrent neural network for real-time speech enhancement," in *Interspeech*, 2018, pp. 3229–3233.
- [15] T. Gao, J. Du, L.-R. Dai, and C.-H. Lee, "SNR-Based Progressive Learning of Deep Neural Network for Speech Enhancement," in *INTERSPEECH*, 2016, pp. 3713–3717.
- [16] A. Li, C. Zheng, and X. Li, "Convolutional Recurrent Neural Network Based Progressive Learning for Monaural Speech Enhancement," *arXiv preprint arXiv:1908.10768*, 2019.
- [17] A. Li, C. Zheng, R. Peng, and X. Li, "A Time-domain Monaural Speech Enhancement with Recursive Learning," *arXiv preprint arXiv:2003.09815*, 2020.
- [18] S. Anderson, T. White-Schwoch, A. Parbery-Clark, and N. Kraus, "A dynamic auditory-cognitive system supports speech-in-noise perception in older adults," *Hearing research*, vol. 300, pp. 18–32, 2013.
- [19] N. Ballas, L. Yao, C. Pal, and A. Courville, "Delving deeper into convolutional networks for learning video representations," *arXiv preprint arXiv:1511.06432*, 2015.
- [20] O. Oktay, J. Schlemper, L. L. Folgoc, M. Lee, M. Heinrich, K. Mi-sawa, K. Mori, S. McDonagh, N. Y. Hammerla, B. Kainz *et al.*, "Attention u-net: Learning where to look for the pancreas," *arXiv preprint arXiv:1804.03999*, 2018.
- [21] O. Ronneberger, P. Fischer, and T. Brox, "U-net: Convolutional networks for biomedical image segmentation," in *International Conference on Medical image computing and computer-assisted intervention*. Springer, 2015, pp. 234–241.
- [22] S. Ioffe and C. Szegedy, "Batch Normalization: Accelerating Deep Network Training by Reducing Internal Covariate Shift," in *International Conference on Machine Learning*, 2015, pp. 448–456.
- [23] D.-A. Clevert, T. Unterthiner, and S. Hochreiter, "Fast and accurate deep network learning by exponential linear units (elus)," *arXiv preprint arXiv:1511.07289*, 2015.
- [24] H. Noh, S. Hong, and B. Han, "Learning deconvolution network for semantic segmentation," in *Proceedings of the IEEE international conference on computer vision*, 2015, pp. 1520–1528.
- [25] H. Zheng, Z. Yang, W. Liu, J. Liang, and Y. Li, "Improving deep neural networks using softplus units," in *2015 International Joint Conference on Neural Networks (IJCNN)*. IEEE, 2015, pp. 1–4.
- [26] J. S. Garofolo, L. F. Lamel, W. M. Fisher, J. G. Fiscus, and D. S. Pallett, "DARPA TIMIT acoustic-phonetic continuous speech corpus CD-ROM. NIST speech disc 1-1.1," *NASA STI/Recon technical report n*, vol. 93, 1993.
- [27] D. P. Kingma and J. Ba, "Adam: A method for stochastic optimization," *arXiv preprint arXiv:1412.6980*, 2014.
- [28] I.-T. Recommendation, "Perceptual evaluation of speech quality (PESQ): An objective method for end-to-end speech quality assessment of narrow-band telephone networks and speech codecs," *Rec. ITU-T P. 862*, 2001.
- [29] C. H. Taal, R. C. Hendriks, R. Heusdens, and J. Jensen, "A short-time objective intelligibility measure for time-frequency weighted noisy speech," in *2010 IEEE international conference on acoustics, speech and signal processing*. IEEE, 2010, pp. 4214–4217.